



Research article

An experimental study on ultrasonic machining of Tungsten carbide-cobalt composite materials

Ravinder Kataria *, Ravi Pratap Singh, and Jatinder Kumar

Department of Mechanical Engineering, National Institute of Technology Kurukshetra, Haryana, India

* **Correspondence:** Email: kataria.ravinder07@gmail.com; ravinder_1438@nitkkr.ac.in.

Abstract: In current study, the effects of numerous process parameters such as properties of work material, profile of tool, grit size, tool feed rate and power rating on rate of material removal and tool wear have been investigated in ultrasonic machining of WC-Co composite material. Taguchi's L-18 orthogonal array has been utilized for planning the experiments. Analysis of variance (ANOVA) is also utilized to find the significant factors. Multi-response optimization has been done by using grey relation analysis (GRA) method. Tool with square type profile carries better performance for material removal rate. Significant effects are observed for process variables such as tool profile, abrasive grain size, power level and tool feed rate. Obtained results have been found to corroborate with confirmatory experimental results.

Keywords: ANOVA; GRA; machining; MRR; optimization; Taguchi; TWR; USM; WC-Co

1. Introduction

WC-Co composite is classed among the most important metal matrix composite materials manufactured by a process called as "powder metallurgy". The several steps included in the production of WC-Co composite are; making of tungsten carbide powder, consolidation of the powder, sintering in the liquid phase followed by post-sintering operations. WC-Co composite materials are also known as cermets, hard metal and cemented carbide [1]. WC-Co composites are hard materials with high mechanical strength (excellent hardness, wear resistance) and better dimensional stability. Due to these superior properties, these have widespread applications in

industry, e.g., manufacturing of wear parts, die and punch manufacturing and cutting and drilling tools.

WC-Co material has high strength, hardness, and superior wear resistance and it has high melting temperature. Due to these properties, it becomes quite difficult to process this material. Machining of WC-Co has been reported by using different processes (such as; turning, Electric discharge machining (EDM), Wire EDM and powder mixed EDM) by the different investigators which resulted in high cutting force, high surface roughness and surface defects (cracks, heat effected zone, recast layer). These defects result in decrease in corrosion resistance of machined surface, wear resistance, hardness and also affect the product quality [1–9]. A number of studies have also reported the application of contemporary machining practices such as EDM, wire EDM, etc. However, problems caused by the different physical characteristics of WC and Co (such as melting point, thermal conductivity) have been reported; mainly in terms of dislodging of WC grains, agglomeration of graphite (carbon) and WC grains. These problems usually lead to the loss of process stability and arcing phenomenon during machining. The topography and integrity of the surface generated after machining is also affected.

Ultrasonic machining is a contemporary manufacturing method usually employed for processing materials with higher hardness/brittleness such as quartz, semiconductor materials, ceramics etc [10,11]. Kumar et al. [11] evaluated the machining characteristics in terms of surface roughness (SR), tool wear rate (TWR) and material removal rate (MRR) at different level of input parameters in ultrasonic machining of titanium. Results reported that, all parameters are significant for MRR and TWR, and SR was considerably influenced by grit size. Kataria et al. [12] investigated SR of machined surface of WC-Co and results shows that grit size was the most significant factor. Kataria et al. [13] reported that power rating and grit size are the factors of high significance which affect the cutting ratio, overcut and taper angle. Jadoun et al. [14] optimized the process parameter for cutting ratio in ultrasonic machining of alumina ceramic. Cutting ratio increases while increasing the power rating and decreasing the abrasive grit size.

Hocheng et al. [15] reported the influence of amplitude and static load on machinability in ultrasonic drilling of ceramics (Zirconia based). Komaraiah and Reddy [16], Jianxin and Taichiu [17], and Kumar and Khamba [18] assessed the impact of work material properties on machining characteristics in ultrasonic machining. Results reported that work materials with higher fracture toughness and hardness tend to be machined at higher removal rates. Teimouri et al. [19] performed the multi response optimization using imperialist competitive algorithm (ICA). Lalchhuanvela et al. [20] explored the effect of USM process parameters on MRR and SR while machining alumina ceramic. Results reported that the maximum MRR could be attained at higher level of every input parameter and SR decreases with decrease in grit size and power rating. Adithan et al. [21] studied the tool wear characteristics and showed that the stainless steel tool had low tool wear as compared to tungsten carbide and mild steel. Table 1 presents an overview of the research content of previously reported studies on ultrasonic machining.

Ultrasonic machining could be a potential solution for addressing the problems related to machinability of WC-Co material. The machined surface produced by USM does not carry any surface defects (cracks, recast layer, heat effected zone etc.) which is generally found in thermal based processes [22]. Therefore, an attempt has been made to further explore the machining efficiency in ultrasonic drilling of WC-Co composites. In the reported literature, very few investigators used the different types of tool profiles, tool feed rate as process parameters for their

investigation. Moreover, few studies were reported on multi-response optimization problem. Thus, the current article is aimed to study the effect of tool profile, tool feed rate on MRR and TWR, by coupling these parameters with other critical, unexplored variables such as content of Cobalt constituent (in work material), power rating and grit size. An appraisal of independent effects of the input variables has been made and optimal parametric settings are identified. Grey relation analysis has been utilized for devising the multi-response optimization.

Table 1. An overview of different profiles of drilled hole and objectives considered in previous studies and present study.

S. No.	Author	Work material	Profile of drilled hole	Objective considered			Optimization
				MRR	TWR	SR	
1.	R. S. Jadoun, Pradeep Kumar, B. K. Mishra, R. C. S. Mehta [23]	Ceramic composites	○	✗	✓	✗	SRO
2.	Deng Jianxin, Lee Taichiu [17]	Alumina-based ceramic composites		✓	✗	✓	SRO
3.	Jatinder Kumar, J.S. Khamba [24]	Titanium (ASTM Grade I)	○	✗	✓	✓	SRO
4.	Vinod Kumar, J. S. Khamba [25]	Stellite 6 (Cobalt alloy)	○	✓	✓	✗	MRO
5.	Vinod Kumar, J. S. Khamba [26]	Alumina-based ceramic composites	○	✓	✗	✓	SRO
6.	H. Lalchuanvela, Biswanath Doloi, B. Bhattacharyya [20]	Alumina ceramic	⬡	✓	✗	✓	MRO
7.	Jatinder Kumar, J.S. Khamba [18]	HCS, HSS Aluminium, Titanium, Carbide Glass	○	✓	✓	✗	SRO
8.	Rupinder Singh, J. S. Khamba [27]	Titanium (ASTM Gr.2) and Titanium (ASTM Gr.5)	○	✗	✓	✗	SRO
9.	Vinod Kumar, J. S. Khamba [28]	Tungsten carbide	○	✓	✗	✓	SRO
10.	Present study	WC-6%Co and WC-24%Co	○ □ △	✓	✓	✗	MRO

✓ = Considered, ✗ = Not Considered, ○ = Round, ⬡ = Hexagonal, □ = Square, △ = Triangle,
SRO = Single response optimization, MRO = Multi-response optimization.

2. Materials and Methods

The fabrication of WC-Co composite includes several steps; production of tungsten metal powder, blending, ball milling, drying, powder compaction process. At last, sintering is performed for obtaining the machining samples in compact form.

The scanning electron microscopy (SEM) and energy dispersive X-ray (EDX) was also employed in a view to characterize WC-Co composite material. ASTM E3 standards were followed for preparation of composites samples. The microstructure of composite (with 6% cobalt) is depicted in Figure 1(A). The uniformly distribution of cobalt particles can be observed throughout the matrix. Figure 1(B) depicts the surface topography of the sample of composite with 24% Cobalt. The uniformly distribution of cobalt particles can be observed throughout the matrix. The EDX analysis confirmed about the composition of WC and Co grains in the machining samples, as shown in Figure 2.

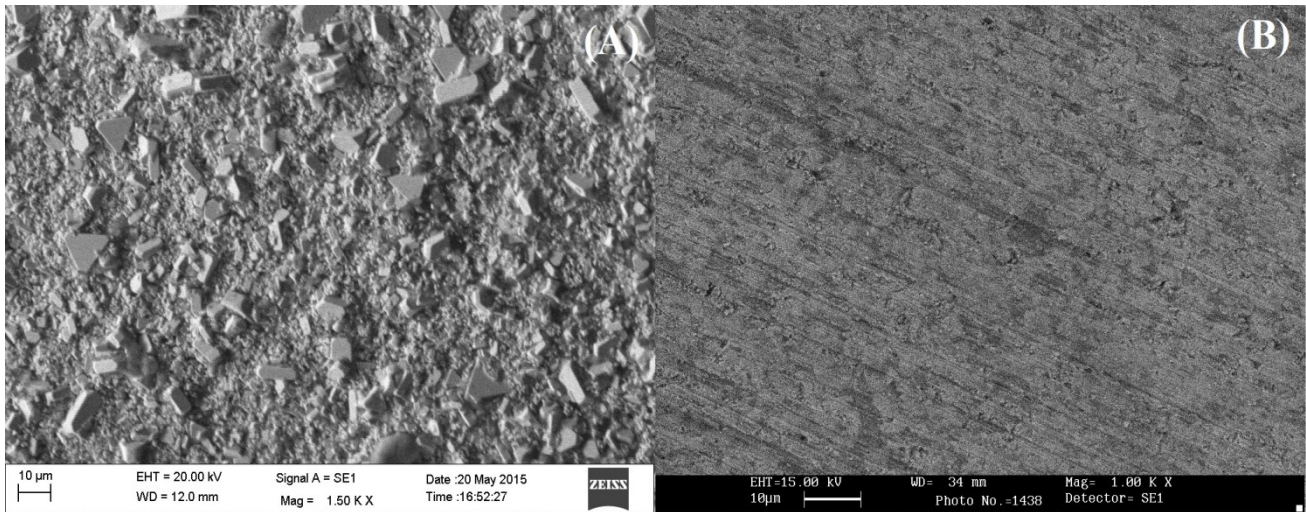


Figure 1. Microstructure of composite with 6%Co (1500 \times); (B) Microstructure of composite with 24%Co obtained by SEM (1000 \times).

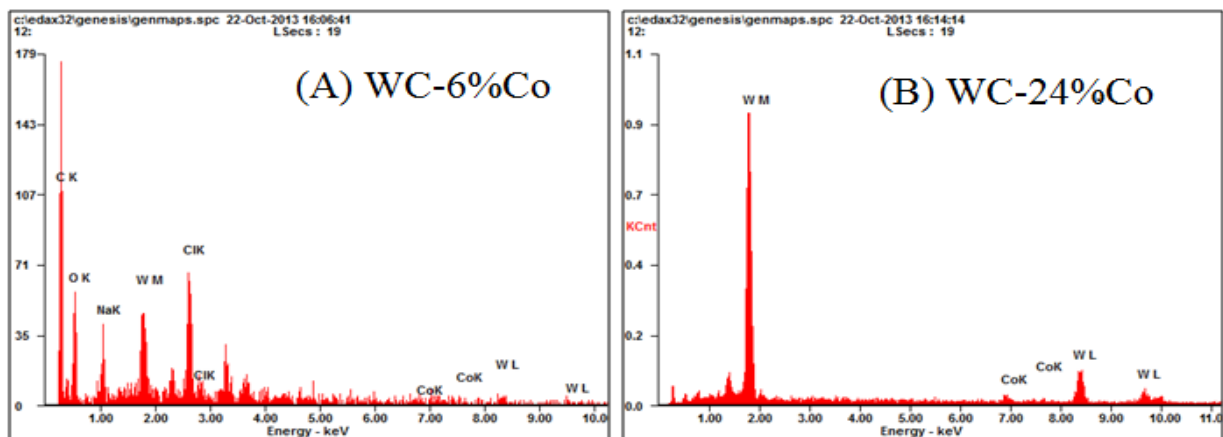


Figure 2. EDX spectrum (before machining) of WC-Co composites.

In the present study WC-Co composite material having 6% and 24% cobalt content has been taken as work material (diameter 20 mm and thickness 3 mm). The chemical and mechanical properties are shown in Table 2. The selection of tool profiles was made randomly. The composition was considered with a broad variation in cobalt content so as to obtain the effect of work material properties (such as fracture toughness, hardness) appropriately. The tool feed rate was selected on the basis of machine operating range (low, medium, and high). Grit size was selected as per the available literature. The range of power rating was selected on the basis of pilot experimentation results. Past literature shows that hollow tools gives better performance as compared to solid tools [18]. So, hollow tools were selected for present experimentation. These tools are having better inertia and efficient flow of abrasive slurry. Stainless steel material is selected as tool material with three different profiles; round, triangular, square having same cross-sectional area. Figure 3 shows the detailed drawing of round and square tool. Three types of grit sizes (200, 320 and 500) of boron carbide are used for preparation of abrasive slurry for the experimentation. Power rating and feed rate at three levels were selected for this work. Table 3 illustrates the different input parameters along with their levels.

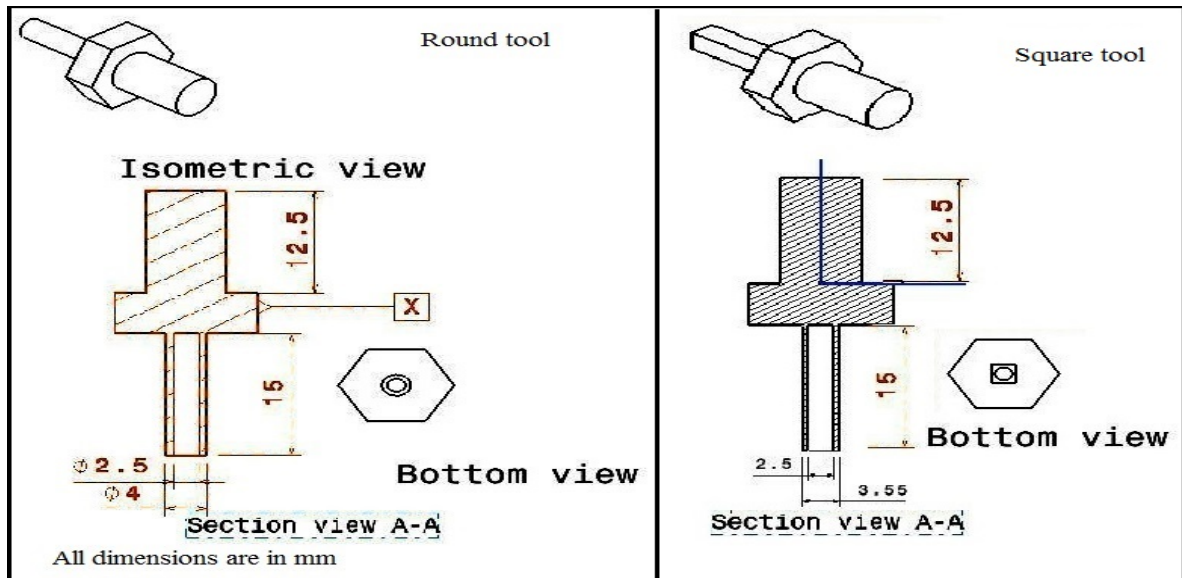


Figure 3. Detailed drawing of round and square tool.

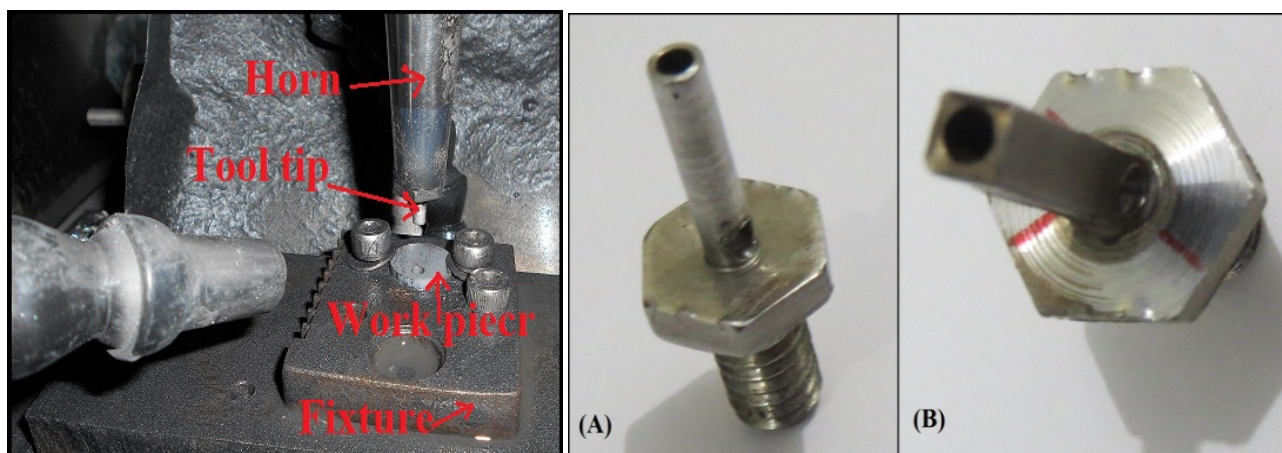
Table 2. Mechanical properties and chemical composition of WC-Co composites.

		WC-6%Co	WC-24%Co
Chemical composition	WC	94%	76%
	Co	6%	24%
Mechanical properties	Density (g/cm ³)	14.9	12.9
	Hardness (HV ₃₀)	1580	780
	Elastic modulus (GPa)	630	470
	Fracture toughness (MPa·√m)	9.6	14.5
	Thermal conductivity (W/mK)	80	50
Thermal expansion of coefficient (×10 ⁻⁶ /K)		5.5	7.5

Table 3. Input factors and their levels (with coded units).

Symbol	Parameter	Level 1	Level 2	Level 3	Units
A	Cobalt content	6% (+1)	24% (-1)		
B	Profile of tool	Round (-1)	Triangular (0)	Square (+1)	
C	Grit size	200 (+1)	320 (0)	500 (-1)	grit no.
D	Power rating	40% (-1)	60% (0)	80% (+1)	watt
E	Tool feed rate	0.015 (+1)	0.018 (0)	0.021 (-1)	mm/s
Constant parameter					
Frequency of vibration	20 kHz	Slurry flow rate	50 × 10 ³ mm ³ /min		
Static load	1.63 kg	Abrasive material	Boron carbide		
Amplitude of vibration	25.3–25.8 μm	Slurry medium	Water		
Slurry concentration	25%	Tool material	Stainless steel		
Slurry temperature	24 °C				

The experiments were performed on an “AP-450 model” (Sonic-Mill, Albuquerque, USA). Figure 4 shows machining zone and pictorial view of tools used. Material removal rate is measured by taking the mass of the metal removed during machining, divided by time taken for machining to the required depth. Time taken for each experiment was recorded by stop watch. The weight was measured with an electronic balance whose least count was 0.0001 g. In same way, tool wear rate was calculated.

**Figure 4.** Illustration of machining zone in USM and tool profiles (A: Round; B: Square).

This study makes use of Taguchi’s L-18 OA for design of the experimental plan. It includes four factors with three levels and one factor has two levels. The total dof associated with five parameters is $9 \times (1 \times 1 + 2 \times 4)$. Hence, L-18 OA was selected for the present study (with dof 17).

Experiments were performed as per L-18 array (as shown in Table 4). Each trial was replicated twice. In order to reduce experimental error, all 54 trials were conducted in completely randomized fashion. The design matrix and experimental results are briefed in Table 4.

Table 4. Design matrix based on L-18 OA (in coded unit) and experimental results.

Exp No.	A	B	C	D	E	Material removal rate		Tool wear rate		Normalized value		GRC		GRG
						Average	S/N	Average	S/N	MRR	TWR	MRR	TWR	
						(g/min)	(dB)	(g/min)	(dB)					
1	+1	-1	+1	-1	+1	0.0153	-36.39	0.0035	49.04	0.356	0.708	0.437	0.631	0.534
2	+1	-1	0	0	0	0.0214	-33.40	0.0048	46.04	0.495	0.559	0.497	0.532	0.515
3	+1	-1	-1	+1	-1	0.0330	-29.64	0.0073	42.64	0.670	0.391	0.602	0.451	0.527
4	+1	0	+1	-1	0	0.0145	-36.96	0.0029	50.51	0.329	0.780	0.427	0.695	0.561
5	+1	0	0	0	-1	0.0386	-28.27	0.0051	45.77	0.733	0.546	0.652	0.524	0.588
6	+1	0	-1	+1	+1	0.0353	-29.04	0.0071	42.83	0.697	0.400	0.623	0.455	0.539
7	+1	+1	+1	0	+1	0.0423	-27.47	0.0064	43.79	0.770	0.448	0.685	0.475	0.580
8	+1	+1	0	+1	0	0.0718	-22.88	0.0105	39.50	0.984	0.236	0.968	0.395	0.682
9	+1	+1	-1	-1	-1	0.0203	-33.87	0.0045	46.83	0.473	0.598	0.487	0.554	0.521
10	-1	-1	+1	+1	-1	0.0896	-20.94	0.0173	35.23	1.074	0.025	1.172	0.339	0.756
11	-1	-1	0	-1	+1	0.0080	-42.05	0.0018	54.64	0.093	0.984	0.355	0.970	0.663
12	-1	-1	-1	0	0	0.0121	-38.44	0.0024	52.06	0.261	0.857	0.403	0.778	0.591
13	-1	0	+1	0	-1	0.0293	-30.71	0.0062	44.08	0.620	0.462	0.568	0.482	0.525
14	-1	0	0	+1	+1	0.0235	-32.56	0.0051	45.61	0.534	0.538	0.518	0.520	0.519
15	-1	0	-1	-1	0	0.0064	-44.05	0.0017	54.95	0.000	1.000	0.333	1.000	0.667
16	-1	+1	+1	+1	0	0.0748	-22.53	0.0183	34.73	1.000	0.000	1.000	0.333	0.667
17	-1	+1	0	-1	-1	0.0185	-34.74	0.0043	47.18	0.433	0.616	0.468	0.565	0.517
18	-1	+1	-1	0	+1	0.0072	-42.92	0.0022	52.72	0.053	0.890	0.345	0.819	0.582

3. Experimentation and Data Collection

In Taguchi method, the variation inherent in performance characteristic is represented by S/N ratio. The terms “signal” and “noise” represents desirable (mean) and undesirable value (standard deviation) respectively. In accordance to Taguchi, the response variables are categorized into two different types, e.g. larger the best (LTB) and smaller the best (STB) [29]. Following relations are utilized for assessment of the S/N ratio;

Larger the best

$$\left(\frac{S}{N}\right)_{LB} = -10 \log \left(\frac{1}{R} \sum_{j=1}^R \frac{1}{y_j^2} \right) \quad (1)$$

Smaller the best

$$\left(\frac{S}{N}\right)_{SB} = -10 \log \left(\frac{1}{R} \sum_{j=1}^R y_j^2 \right) \quad (2)$$

where y_j is the response value recorded in j^{th} observation. Here, for MRR, “larger the best” and for TWR, “smaller the best” type S/N ratio were computed. Minitab-16 software has been utilized for analyzing the results.

4. Results and Discussions

MRR and TWR have been studied under the influence of each parameter. Figure 5 illustrates the normal probability plots of residuals for MRR and TWR. Normal distribution of errors has also been revealed as almost all of the residual values are observed to fall on the fitted curve. Hence, Model assumptions are being validated for analysis of variance (ANOVA) test.

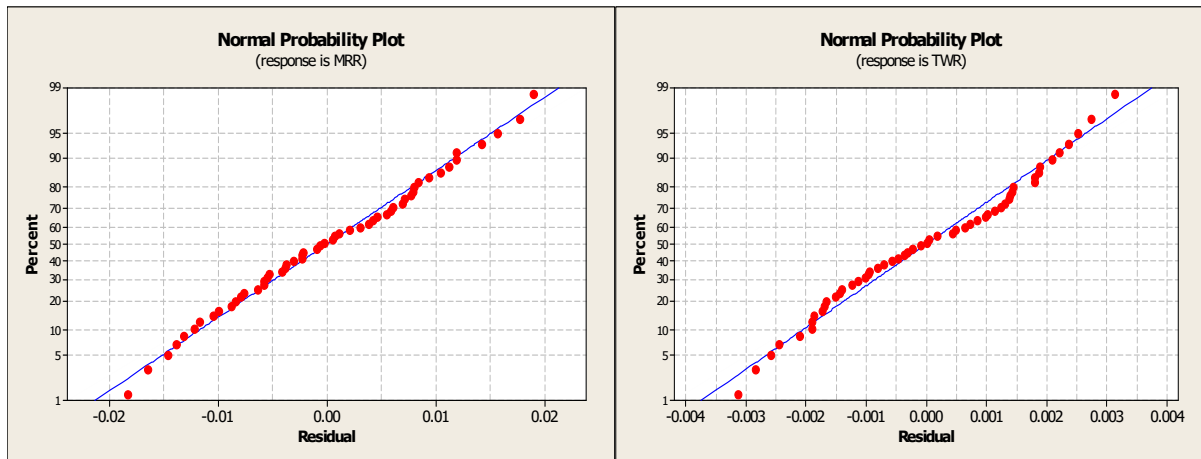


Figure 5. Normal probability plot for MRR and TWR.

4.1. Material Removal Rate

Figure 6 shows that increase in cobalt content results in lower value of MRR. It happens because as cobalt content increases, the fracture toughness increases. Hence the crack propagation and intersection become difficult and requires more energy which results in reduced MRR. Tool profiles have significant effect on the MRR. Square tool profile gives higher MRR as compared to round and triangular tool profiles. This may be related to the efficient flow of slurry particles under the square shaped tool.

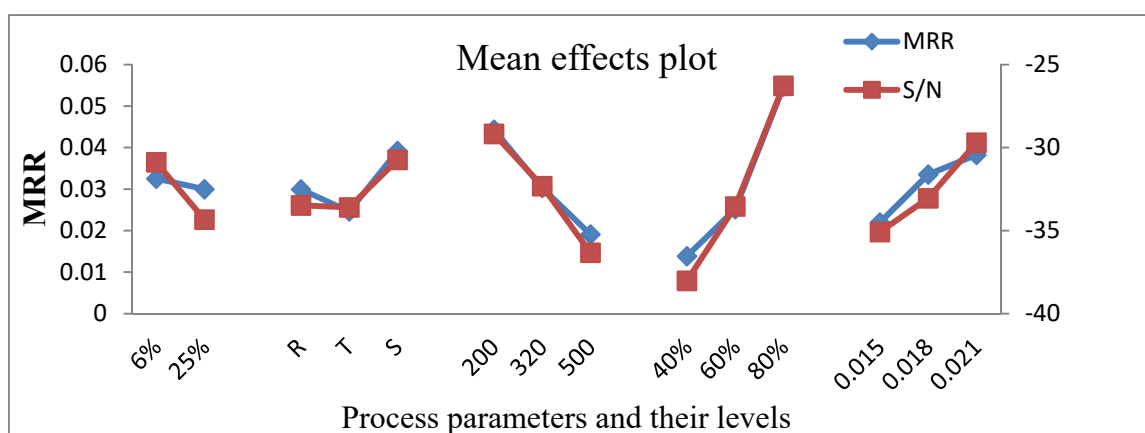


Figure 6. Mean effect plots for MRR.

As coarseness of the abrasive grains increases, MRR also increases. There are mainly two wear mechanisms (hammering action and throwing action) given for the USM process, as reported in literature. Hammering of the grains on the surface is considered as primary wear mechanism. Increasing the grit size causes the reduction in surface density of abrasive particles, which further results into an immense growth of the resultant stress due to action of each grit particle. This results into increase of material removal rate. As grit size increases, the mass of the particles also increases, which results into greater impact force (per unit area). Thus, in both cases, the effective stress on the surface of the work sample is increased with the grit size, which accelerates the micro-chipping and hence the material removal. These results are found consistent with the findings of the other researchers [11,18,20]. Power rating is also a significant process parameter in ultrasonic machining of WC-Co composite. An increment in power rating produces a significant improvement in machining rate. Increased power rating results in increase of amplitude of vibration, thereby increasing the abrasive grit particles momentum before making impact. Higher energy of abrasive particles results into the removal of larger lumps from surface of work material, which is responsible for the increasing MRR. Similar results were reported in previously published investigations [18,24]. Tool feed rate also affects the material removal rate. Rate of increase in MRR is higher for feed rate from 0.015 to 0.018, while it is slower for feed rate value from 0.018 to 0.021. Overall increase in tool feed rate gradually increases the MRR. The S/N ratio is found to be highest at these levels, which signals the maximization of the desired value of the response with minimum impact of noise.

ANOVA test is also performed for raw data and S/N ratio data in order to evaluate the significant parameters that contribute to the variation in MRR and also to evaluate the percentage wise contribution. Tables 5 and 6 show the ANOVA results for raw data and S/N data respectively. Results from ANOVA test (raw data) depict that the descending order of various factors as per their significance for MRR as-power rating (52.06%), grit size (18.70%), tool feed rate (8.20%), and tool profile (6.34%). However the contribution of process parameters from the ANOVA test (S/N ratio data) is as follows; power rating (52.51%), grit size (19.24%), tool feed rate (11.01%), cobalt content (6.60%) and tool profile (3.92%).

MRR is “larger the best” type response. Thus, the higher value of MRR is considered as desirable. As described in Figure 6, the optimal process setting for MRR is as; first level of cobalt content (A1), profile of tool at third level (B3), grit size at first level (C1), power rating at third level (D3), and third level of tool feed rate (E3).

Table 5. ANOVA for MRR (raw data).

Source	dof	Seq. SS	Adj. SS	Adj. MS	F	P
A	1	0.0001	0.0001	0.0001	0.87	0.356
B	2	0.0019	0.0019	0.0009	9.68	0.000
C	2	0.0057	0.0057	0.0028	28.55	0.000
D	2	0.0160	0.0160	0.0080	79.51	0.000
E	2	0.0025	0.0025	0.0012	12.53	0.000
Error	44	0.0044	0.0044	0.0001		
Total	53	0.0307				

A—cobalt content, B—profile of tool, C—grit size, D—power rating, E—feed rate

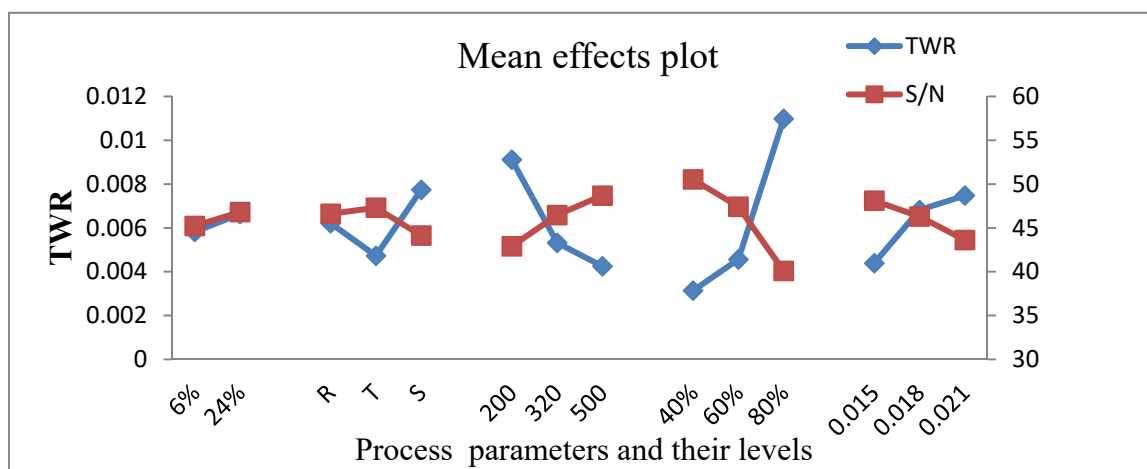
Table 6. ANOVA for MRR (S/N data).

Source	dof	Seq. SS	Adj. SS	Adj. MS	F	P
A	1	53.4	53.4	53.4	8.0	0.022
B	2	31.5	31.5	15.7	2.3	0.157
C	2	154.5	154.5	77.2	11.5	0.004
D	2	421.8	421.8	210.9	31.5	0.000
E	2	88.4	88.4	44.2	6.6	0.020
Error	8	53.4	53.4	6.6		
Total	17	803.2				

4.2. Tool Wear Rate

Figure 7 depicts that tool wear rate is not affected by cobalt content significantly. Tool with square profile exhibit more TWR as compared to round and triangular type profiles; as observed from raw data and S/N ratio data. Abrasive grit size also has significant effect on TWR. TWR increases as abrasive grit size increases. Use of grains of larger diameter results in large micro cavities on the surface of the tool, which is responsible for higher tool wear rate. These results are found to be consistent with previously reported researches [18,30]. It is also observed that, TWR is higher at that combination of grit size and power level which yields higher MRR.

It is observed that an increase in power rating results into higher TWR. As power rating increases, high energy abrasive grit particles strike the surface of tool which creates hasty cracking in the tool surface, thus encouraging tool wear rate. Similar results also suggested by Jadoun, et al. [23] and, Kumar and Kumar [30]. Tool feed rate is also significant for TWR. Increase in tool feed rate corresponds to increase in tool wear rate. Rate of increase in TWR is higher for feed rate ranges from 0.015 to 0.018, while it is slower for feed rate value from 0.018 to 0.021. In other words, TWR gradually increases with an increase in tool feed rate. When considering S/N response, the highest value signals the optimal level of each parameter, which corroborates the results of mean response. However, cobalt content in work material is following a different trend as compared to other variables.

**Figure 7.** Mean effect plots for TWR.

ANOVA test was also performed to evaluate significant factors for TWR and also to evaluate the percentage wise contribution. ANOVA results for raw data and S/N data are presented in Tables 7 and 8. Results from ANOVA test (raw data) show that the descending order of various factors as per their significance for TWR as-power rating (52.98%), grit size (19.82%), tool feed rate (8.01%), and tool profile (6.87%). However, the contribution of process parameters from the ANOVA test (S/N ratio data) is as follows; power rating (58.98%), grit size (17.46%), tool feed rate (10.47%), tool profile (5.71%), and cobalt content (1.93%).

Table 7. ANOVA for TWR (raw data).

Source	dof	Seq. SS	Adj. SS	Adj. MS	F	P
A	1	0.00001	0.00001	0.00001	2.8	0.100
B	2	0.00008	0.00008	0.00004	13.1	0.000
C	2	0.00023	0.00023	0.00011	37.7	0.000
D	2	0.00062	0.00062	0.00031	100.7	0.000
E	2	0.00009	0.00009	0.00004	15.2	0.000
Error	44	0.00013	0.00013	0.00000		
Total	53	0.00118				

Table 8. ANOVA for TWR (S/N data).

Source	dof	Seq. SS	Adj. SS	Adj. MS	F	P
A	1	11.3	11.3	11.3	2.8	0.130
B	2	33.3	33.3	16.6	4.2	0.057
C	2	101.9	101.9	50.9	12.8	0.003
D	2	344.2	344.2	172.1	43.3	0.000
E	2	61.1	61.1	30.5	7.7	0.014
Error	8	31.8	31.8	3.9		
Total	17	583.6				

TWR is “smaller the best” type response. So, the lowest value of TWR is considered as desirable. As described in Figure 7, the optimal process setting for TWR is as; cobalt content at first level (A1), second level of tool profile (B2), grit size at third level (C3), power rating at first level (D1), and first level of tool feed rate (E1). Percentage contribution of different factors on MRR (raw data) and TWR (raw data) is depicted in Figure 8.

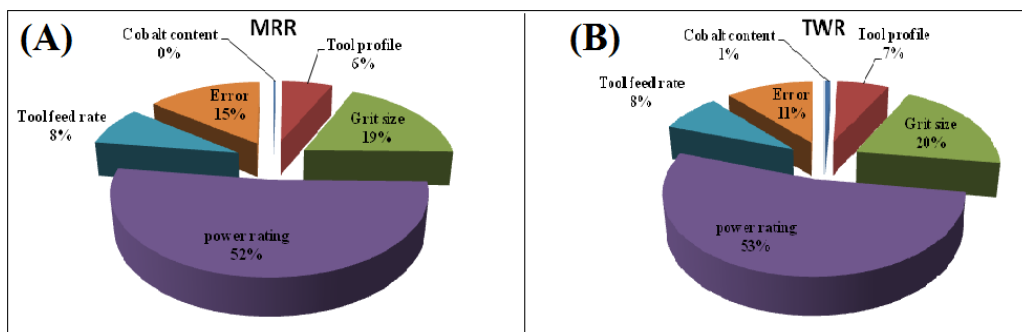


Figure 8. Percentage wise contribution of factors on (A) MRR; (B) TWR.

Table 9 shows the macro-model for MRR and TWR. The macro-model is generated by the application of Taguchi's single response optimization.

Table 9. Macro-model for MRR and TWR.

For MRR	
Work material	6% cobalt content
Tool profile	Square
Grit size	200 mesh
Power rating	80%
Tool feed rate	0.021 mm/s
For TWR	
Work material	6% cobalt content
Tool profile	Triangular
Grit size	500 mesh
Power rating	40%
Tool feed rate	0.015 mm/s

4.3. Prediction of Mean

The prediction of optimal performance and depiction of confidence interval has been achieved by employing Taguchi approach. The results obtained from confirmatory experiments must lie in the confidence interval ($\alpha = 0.05$).

Following equation has been used to compute CI_{CE} and CI_{POP} [29].

$$CI_{CE} = \sqrt{Fa(1, fe)Ve \left[\frac{1}{n_{eff}} + \frac{1}{R} \right]} \quad (3)$$

$$CI_{POP} = \sqrt{Fa(1, fe)Ve \left[\frac{1}{n_{eff}} \right]} \quad (4)$$

Where $Fa(1, fe)$ = the F ratio at a confidence level of against dof 1, and error dof f_e ;

$$n_{eff} = \frac{N}{1 + [Total\ DOF\ associated\ in\ the\ estimate\ of\ the\ mean]};$$

N = Total number of results;

R = No. of replications;

V_e = Error variance

Table 10 represents the predicted values, experimental results at optimized setting.

The correlation of MRR and TWR has been established through quadratic regression. The best fitting line for prediction of tool wear rate (over a range of material removal rate) was revealed using MINITAB 16 software (as shown in Figure 9). The quadratic regression equation from the least squares line is:

$$TWR = 0.001258 + 0.1278 \text{ MRR} + 0.6320 \text{ MRR}^2 \quad (5)$$

Using this equation, tool wear rate can be estimated for a given value of MRR. The value of R-sq is close to unity (.909); hence the degree of correlation among the two response variables (MRR, TWR) is high. In another words, higher MRR cannot be obtained without accepting a higher magnitude of TWR. Hence, the higher productivity is obtained at the cost of machining economy.

Table 10. Predicted and experimental results at optimized setting.

Performance characteristic	Optimized setting	Predicted Values (g/min)	Experimental Results (g/min)	Confidence intervals	
MRR	A1B3C1D3E3	0.0418	0.0335 g/min	CI _{CE}	$0.0273 < \mu_{\text{MRR}} < 0.0563$
				CI _{POP}	$0.0331 < \mu_{\text{MRR}} < 0.0563$
TWR	A1B2C3D1E1	0.0044	0.0052 g/min	CI _{CE}	$0.0019 < \mu_{\text{TWR}} < 0.0070$
				CI _{POP}	$0.0029 < \mu_{\text{TWR}} < 0.0060$

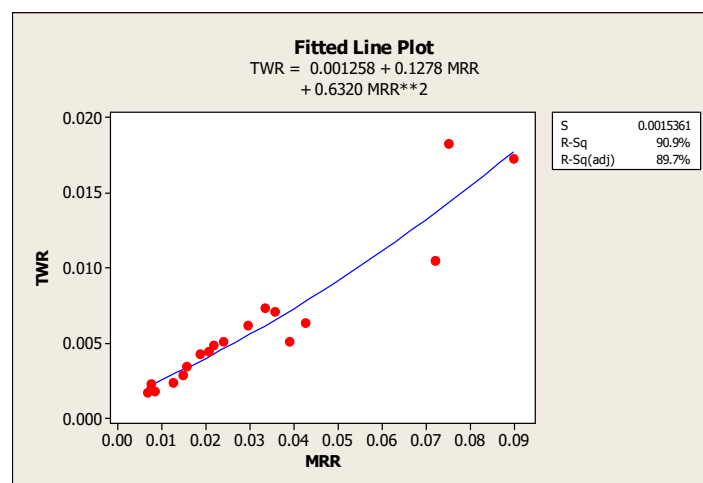


Figure 9. Correlation between MRR and TWR.

4.4. Multi-response Optimization using GRA Method

Grey relation analysis is an effective method used for solving the multi response optimization problems. GRA method can also be used for solving the complicated interrelationship among the data when the trends of their development are either homogeneous or heterogeneous. The major advantages of GRA method are; results based on real data, computations are simpler and apparent, and it is also one of the excellent techniques employed to build decisions in manufacturing milieu [31]. The simultaneous optimization of the investigated machining responses makes the process applicability more meaningful while tackling real life industrial problems [32,33]. This method includes the evaluation of multi-response based on grey relational grade (GRG). Therefore, a multiple response optimization can be performed by converting it into single response optimization by using GRG. The multi-response optimization is done by treating GRG as an overall evaluation of experimental data. Optimize value of a process parameter is related to GRG at highest level. The procedure for computation of GRG value for different trials and depiction of optimized process situation can be illustrated as follows [34]:

Step 1: Values of SN ratio are computed for each objective for all the trials using Eqns. (1)–(2).

Step 2: Values of SN ratio are normalized for all the process objectives employing Eqn.

$$Z_{jys} = \frac{Z_{yi} - \min Z_{yi}}{\max Z_{yi} - \min Z_{yi}} \quad (6)$$

where $\min Z_{yi} = \min \{Z_{1yi}, Z_{2yi}, \dots, Z_{myi}\}$ and $\max Z_{yi} = \max \{Z_{1yi}, Z_{2yi}, \dots, Z_{myi}\}$

Step 3: Calculate grey relational coefficients (GRC) of each response for all trials.

The GRC (γ_{jy}) for y^{th} response in j^{th} trial can be calculated as below:

$$\gamma_{jy} = \frac{\Delta_y^{\min} + \xi \Delta_y^{\max}}{\Delta_{jy} + \xi \Delta_y^{\max}} \quad (7)$$

where $\Delta_{jy} = |1 - Z_{jys}|$, $\Delta_y^{\min} = \min\{\Delta_{1y}, \Delta_{2y}, \dots, \Delta_{my}\}$, $\Delta_y^{\max} = \max\{\Delta_{1y}, \Delta_{2y}, \dots, \Delta_{my}\}$ and ξ is the distinguishing coefficient ($\xi \in [0,1]$, it is set equal to 0.5).

Step 4: GRG_j corresponding to j^{th} trial calculated as;

$$\text{GRG}_j = \sum_{y=1}^p W_y \gamma_{jy} \quad (8)$$

The weights for MRR and TWR considered as 0.5 and 0.5 respectively to perform the calculations for multi-response optimization.

Step 5: Utilize arithmetic mean to compute the parameters effects on GRG value and then optimal combination is decided by considering higher-the-better factor effects.

Figure 10 shows the main effects plot for GRG, in which optimized setting is found as cobalt content (25%), profile of tool (round), grit size (200), power rating (80%), and feed rate (0.018).



Figure 10. Effects of process variables on grey relational grade.

In case of single response optimization, the predicted S/N ratio for MRR and TWR was found as -18.46 and 55.79 respectively and for multi response optimization these were -22.41 and 38.75 respectively as illustrated in Table 11.

Table 11. Predicted SN ratios for single and multi-response optimization methods.

Optimization Method	Performance characteristics	Optimized Setting	Predicted SN ratio	
			MRR(dB)	TWR(dB)
Single response optimization using Taguchi method	MRR	A1B3C1D3E3	-18.46	---
	TWR	A1B2C3D1E1	---	55.79
Multi response optimization using GRA method	GRG	A2B1C1D3E2	-22.41	38.75

Table 12 illustrates a comparison of results obtained for ultrasonic machining of different materials selected by various investigators in past research work. It is revealed that from the literature that there is a vast range of materials that can be machined with USM. It can also be concluded that most of the responses in USM processes are well affected with the proper selection of process variables. The results presented in current article are somehow differ from past investigations and this can be considered due to the incorporation of some parameters i.e. profile of tool, feed rate etc. which were almost omitted in past literature. Table 13 represents the results obtained in the machining of WC-Co composites with various processes. It is revealed that with USM machined surface is found to be free from any defects such as; heat affected zone, recast layer etc. which are usually occurs in thermal based processes.

Table 12. A comparative presentation of results obtained for different materials machined with USM.

S. no.	Author	Input parameters and range	Work material	Results at optimized setting
1.	Present Study	Cobalt content (6% and 24%) Tool profile (Round, triangular, square) Grit size (200–500 mesh size) Power rating (40%–80%) Tool feed rate (0.015–0.021 mm/s)	WC-6%Co and WC-24%Co	MRR: 0.0335 g/min TWR: 0.0052 g/min Tool profile has significant effect on the MRR and TWR
2.	Jatinder Kumar, Vinod Kumar [30]	Tool (HCS, HSS, Titanium, Ti alloy, Carbide) Abrasive (Al ₂ O ₃ , SiC, B ₄ C) Grit size (220–500 mesh size) Power rating (100–400 W)	Titanium (ASTM Grade I)	TWR: 0.45 mg/min Tool material was most significant factor for TWR.
3.	Vinod Kumar, J. S. Khamba [25]	Tool (Titan12, Titan15, Titan31) Abrasive (Al ₂ O ₃ , SiC, B ₄ C) Slurry conc. (20–30%) Grit size (220–500 mesh size) Power rating (25–75%)	Stellite 6 (Cobalt alloy)	MRR: 0.185 mm ³ /min TWR: 0.064 mm ³ /min
4.	Rupinder Singh, J. S. Khamba [27]	Tool (SS, HSS, Diamond, Titanium, Carbide, HCS) Abrasive (Al ₂ O ₃ , SiC, B ₄ C) Slurry conc. (15–25%) Grit size (220–500 mesh size) Power rating (30–90%)	Titanium (ASTM Gr.2) and Titanium (ASTM Gr.5)	TWR: 8.94 × 10 ⁻³ g/min Tool material, power rating, and slurry grit size significantly affects TWR

5.	Jatinder Kumar, J. S. Khamba, S.K. Mohapatra [35]	Slurry temperature (10–60 °C) Tool (HCS, HSS, Titanium, Ti alloy, Carbide) Abrasive (Al ₂ O ₃ , SiC, B ₄ C) Grit size (220–500 mesh size) Power rating (100–400 W)	Titanium (ASTM Grade I)	MRR: 1.69 mm ³ /min
6.	Ik Soo Kang, Jeong Suk Kim, Yong Wie Seo, Jeon Ha Kim [36]	Tool Cross-section Grit size(240–600 mesh size) Slurry concentration (1:1–1:5) Static Pressure (2–3 kg/cm ²)	Alumina (Al ₂ O ₃) ceramic	MRR: 18.97 mm ³ /min SR: 0.76 μm MRR increased with increase in Slurry conc. For SR grit size is more significant than static pressure.
7.	Jatinder Kumar & J. S. Khamba [37]	Tool (HCS, HSS, Titanium, Ti alloy, Carbide) Abrasive (Al ₂ O ₃ , SiC, B ₄ C) Grit size (220–500 mesh size) Power rating (100–400W)	Titanium (ASTM Grade I)	MRR: 1.67 mm ³ /min TWR: 0.04 mm ³ /min SR: 0.31 μm

Table 13. A comparative presentation of machining performance of present study and other previously reported studies

S. no.	Author	Work Material composition	Process	Results at optimized setting
1.	Present study	WC-6%Co and WC-24%Co	Ultrasonic Machining	MRR: 0.0335 g/min TWR: 0.0052 g/min OR MRR: 2.248 mm ³ /min TWR: .647 mm ³ /min
2.	S. Assarzadeh, M. Ghoreishi [3]	WC-6%Co	Electrical Discharge Machining	MRR: 0.187 mm ³ /min TWR: 0.0381 mm ³ /min SR: 2.48 μm
3.	V.Muthuraman, R. Ramakrishnan [5]	WC-10%Co and WC-20%Co	Wire-Electrical Discharge Machining	MRR: 21.24 mm ³ /min SR: 1.90 μm
4.	A.T.Z Mahamat, A.M.A Rani, P. Husain [6]	WC-6%Co	Electrical Discharge Machining	MRR: 0.007243 g/min EW: 0.0003474 g/min TWR: 0.165370% SR: 3.6 μm
5.	G.K. Singh, V. Yadav, R. Kumar [4]	WC-10%Co	Spark Assisted Diamond Face Grinding	MRR: 0.3845 mm ³ /min WWR: 0.007042 g/min. ASR: 3.606 μm
6.	P. Janmanee, A. Muttamara [2]	WC-10% Co	Electrical Discharge Machining	MRR: 2.731 mm ³ /min EWR: 37.234 mm ³ /min MCD: 183.87 μm/mm ²

5. Conclusions

1. The optimized parametric setting for material removal rate is: work material with cobalt content (6%), profile of tool (square), abrasive grit size (200), power rating (80%), and tool feed rate (0.021 mm/s). The percentage contributions of the various factors in descending order are; power rating (52.06%), grit size (18.70%), feed rate (8.20%), profile of tool (6.34), and cobalt content (0.28%).
2. Power rating is the most significant factor that affects MRR as at high power rating, abrasive material has high impact energy against work surface. It should be noted that highest MRR can be obtained at a combination of high power rating, coarse grit and high feed rate of tool.
3. Profile of tool possesses significant effect on MRR and TWR. For the tools having same cross-section area, square profile tools gives higher MRR and TWR.
4. The optimized parametric setting for tool wear rate is: work material with 6% cobalt content, profile of tool (triangular), abrasive grit size (500), power rating (40%), and tool feed rate (0.015 mm/s). The percentage contributions of the various factors in descending order are; power rating (52.99%), grit size (19.82%), feed rate (8.01%), profile of tool (6.87%), and cobalt content (0.74%). At optimize setting, the predicted S/N ratio was found 55.79 dB.
5. For multi-response optimization, the optimized parametric setting is: work material with 24% cobalt content, profile of tool (round), grit size (200), power rating (80%), and tool feed rate (0.018 mm/s). The predicted S/N ratio for MRR and TWR is -22.41 and 38.75 respectively.
6. MRR and TWR exhibit a strong correlation. Higher MRR can't be obtained without tolerating higher TWR.

Conflict of Interest

The authors declare that there is no conflict of interest regarding the publication of this paper.

References

1. Kataria R, Kumar J (2015) Machining of WC-Co composites—A review. *Mater Sci Forum* 808: 51–64.
2. Janmanee P, Muttamara A (2011) Optimization of electrical discharge machining of composite 90WC-10Co base on Taguchi approach. *Eur J Sci Res* 64: 426–436.
3. Assarzadeh S, Ghoreishi M (2013) Statistical modeling and optimization of process parameters in electro-discharge machining of cobalt-bonded tungsten carbide composite (WC/6%Co). *Procedia Cirp* 6: 464–469.
4. Singh GK, Yadav V, Kumar R (2010) Diamond face grinding of WC-Co composite with spark assistance: Experimental study and parameter optimization. *Int J Precis Eng Man* 11: 509–518.
5. Muthuraman V, Ramakrishnan R (2012) Multi parametric optimization of WC-Co composites using desirability approach. *Procedia Eng* 38: 3381–3390.
6. Mahamat ATZ, Rani AMA, Husain P (2011) Machining of cemented tungsten carbide using EDM. *J Appl Sci* 11: 1784–1790.

7. Yadav SKS, Yadav V (2013) Experimental investigation to study electrical discharge diamond cutoff grinding (EDDCG) machinability of cemented carbide. *Mater Manuf Process* 28: 1077–1081.
8. Bhavsar SN, Aravindan S, Rao V (2012) Machinability study of cemented carbide using focused ion beam (FIB) milling. *Mater Manuf Process* 27: 1029–1034.
9. Mohanty A, Talla G, Gangopadhyay S (2014) Experimental investigation and analysis of EDM characteristics of Inconel 825. *Mater Manuf Process* 29: 540–549.
10. Singh RP, Kumar J, Kataria R, et al. (2015) Investigation of the machinability of commercially pure titanium in ultrasonic machining using graph theory and matrix method. *J Eng Res* 3: 75–94.
11. Kumar J, Khamba JS, Mohapatra SK (2008) An investigation into the machining characteristics of titanium using ultrasonic machining. *Int J Mach Mach Mater* 3: 143–161.
12. Kataria R, Kumar J, Pabla BS (2016) Experimental investigation of surface quality in ultrasonic machining of WC-Co composites through Taguchi method. *AIMS Mater Sci* 3: 1222–1235.
13. Kataria R, Kumar J, Pabla BS (2016) Ultrasonic machining of WC-Co composite material: Experimental investigation and optimization using statistical technique. *P I Mech Eng B-J Eng*.
14. Jadoun RS, Kumar P, Mishra BK, et al. (2006) Optimization of process parameters for ultrasonic drilling (USD) of advanced engineering ceramics using Taguchi approach. *Eng Optimiz* 38: 771–787.
15. Hocheng H, Kuo KL, Lin JT (1999) Machinability of zirconia ceramic in ultrasonic drilling. *Mater Manuf Process* 14: 713–724.
16. Komaraiah M, Reddy PN (1993) A study on the influence of workpiece properties in ultrasonic machining. *Int J Mach Tool Manu* 33: 495–505.
17. Jianxin D, Taichiu L (2002) Ultrasonic machining of alumina based ceramic composites. *J Eur Ceram Soc* 22: 1235–1241.
18. Kumar J, Khamba JS (2009) An investigation into the effect of work material properties, tool geometry and abrasive properties on performance indices of ultrasonic machining. *Int J Mach Mach Mater* 5: 347–366.
19. Teimori R, Baseri H, Moharmi R (2015) Multi-responses optimization of ultrasonic machining process. *J Intell Manuf* 26: 745–753.
20. Lalchhuanvela H, Doloi B, Battacharyya B (2012) Enabling and understanding ultrasonic machining of engineering ceramics using parametric analysis. *Mater Manuf Process* 27: 443–448.
21. Adithan M (1981) Tool wear characteristics in ultrasonic drilling. *Tribol Int* 14: 351–356.
22. Kataria R, Kumar J, Pabla BS (2015) Experimental Investigation into the Hole Quality in Ultrasonic Machining of WC-Co Composite. *Mater Manuf Process* 30: 921–933.
23. Jadoun RS, Kumar P, Mishra BK, et al. (2006) Manufacturing process optimization for tool wear rate in ultrasonic drilling of engineering ceramics using Taguchi method. *Int J Mach Mach Mater* 1: 94–114.
24. Kumar J, Khamba JS (2008) An experimental study on ultrasonic machining of pure titanium using designed experiments. *J Braz Soc Mech Sci* 30: 231–238.
25. Kumar V, Khamba JS (2009) Parametric optimization of ultrasonic machining of co-based super alloy using the Taguchi multi-objective approach. *Prod Eng Res Dev* 3: 417–425.
26. Kumar V, Khamba JS (2006) Experimental investigation of ultrasonic machining of an Alumina-based ceramic composite. *J Am Ceram Soc* 89: 2413–2417.

27. Singh R, Khamba JS (2009) Mathematical modeling of tool wear rate in ultrasonic machining of titanium. *Int J Adv Manuf Tech* 43: 573–580.
28. Kumar V, Khamba, JS (2009) Statistical analysis of experimental parameters in ultrasonic machining of tungsten carbide the Taguchi approach. *J Am Ceram Soc* 91: 92–96.
29. Ross PJ (1996) Taguchi techniques for quality engineering. New York: McGraw–Hill.
30. Kumar J, Kumar V (2011) Evaluating the tool wear rate in ultrasonic machining of titanium using design of experiments approach. *World Acad Sci Eng Tech* 81: 803–808.
31. Kataria R, Kumar J, Pabla BS (2016) Experimental investigation and optimization of machining characteristics in ultrasonic machining of WC-Co composite using GRA method. *Mater Manuf Process* 31: 685–693.
32. Singh RP, Singhal S (2016) Investigation of Machining Characteristics in Rotary Ultrasonic Machining of Alumina Ceramic. *Mater Manuf Process*.
33. Singh RP, Singhal S (2016) Experimental investigation of machining characteristics in rotary ultrasonic machining of quartz ceramic. *P I Mech Eng L-J Mat*.
34. Kataria R, Kumar J (2014) A comparison of the different multiple response optimization techniques for turning operation of AISI O1 tool steel. *J Eng Res* 2: 161–184.
35. Kumar J, Khamba JS, Mohapatra SK (2010) Modelling of the material removal rate in ultrasonic machining of titanium using dimensional analysis. *Int J Adv Manuf Tech* 48: 103–119.
36. Kang IS, Kim JS, Seo YW, et al. (2006) An experimental study on the ultrasonic machining characteristics of engineering ceramics. *J Mech Sci Technol* 20: 227–233.
37. Kumar J, Khamba JS (2010) Multi-response optimization in ultrasonic machining of titanium using Taguchi's approach and utility concept. *Int J Manuf Res* 5: 139–160.



AIMS Press

© 2016 Ravinder Kataria, et al., licensee AIMS Press. This is an open access article distributed under the terms of the Creative Commons Attribution License (<http://creativecommons.org/licenses/by/4.0>)